

Cyclotron motion in graphene

John Schliemann

Institute for Theoretical Physics, University of Regensburg, D-93040 Regensburg, Germany

(Dated: February 11, 2008)

We investigate cyclotron motion in graphene monolayers considering both the full quantum dynamics and its semiclassical limit reached at high carrier energies. Effects of *zitterbewegung* due to the two dispersion branches of the spectrum dominate the irregular quantum motion at low energies and are obtained as a systematic correction to the semiclassical case. Recent experiments are shown to operate in the semiclassical regime.

PACS numbers: 73.63.-b, 73.63.Ad

I. INTRODUCTION

The experimental discovery of graphene, i.e. single layers of graphite, has rapidly led to an extraordinary vast and still growing interest in this material, both experimental and theoretical^{1,2,3}. Compared to conventional two-dimensional electronic systems, the peculiar properties of graphene mainly stem from its linear dispersion near the Fermi energy, and the chiral nature of electronic states entangling the momentum and sublattice degree of freedom^{2,3}. In particular, studies of carrier transport in perpendicular magnetic fields have revealed unusual features like a cyclotron mass being proportional to the square root of the particle density⁴, and, most spectacular, a quantum Hall effect occurring at half-integer filling factors^{4,5,6}. Another partially related feature of graphene is its spectrum of Landau levels being non-equidistant in energy and proportional to the square root of the magnetic field,^{4,5,6,7,8,9} properties also not shared by usual two-dimensional electron gases in semiconductor structures.

In this communication we analyze the cyclotron motion in graphene considering both the full quantum dynamics as well as its semiclassical limit. The latter findings can directly be compared with the results of Shubnikov-de Haas measurements reported on in Ref.⁴. We also comment on a recent preprint by Rusin and Zawadzki studying cyclotron motion in graphene which appeared while the present work was reaching completion¹⁰. These authors concentrate on the full quantum dynamics using a numerical approach analogous to very recent work¹¹ on two-dimensional electron gases in semiconductors, and they stress the role of *zitterbewegung*^{12,13,14,15,16,17,18,19,20,21,22,23,24,25}. As we shall see below, signatures of *zitterbewegung* can also be seen in semiclassical corrections to the classical limit of the underlying quantum dynamics.

In the following section II we investigate the full quantum dynamics of the system using both a numerical and an analytical approach. The latter one is based on the analogy of the Hamiltonian to the Jaynes-Cummings model stemming from quantum optics. This analogy is the starting point for the analysis of the semiclassical limit to be discussed in section III. There we also compare

our results with the Shubnikov-de Haas experiments by Novoselov *et al.*⁴. Section IV contains our conclusions.

II. QUANTUM DYNAMICS

For a graphene sheet in a perpendicular magnetic field, the single-particle states around one of one of the two inequivalent corners of the first Brillouin zone are described by³

$$\mathcal{H} = v(\tau^z \pi_x \sigma^x + \pi_y \sigma^y) \quad (1)$$

with (using standard notation) $\vec{\pi} = \vec{p} + e\vec{A}/c$ and $v \approx 10^6$ m/s. The Pauli matrices describe the sublattice or pseudospin degree of freedom, and the Zeeman coupling to the physical electron spin has been neglected. The label $\tau^z = \pm 1$ determines which corner of the Brillouin zone is considered; in what follows we shall concentrate on $\tau^z = 1$. The Heisenberg equations of motion read

$$\frac{d}{dt} \vec{\pi}_H(t) = \frac{\hbar v}{\ell^2} \vec{\sigma}_H(t) \times \vec{e}_z \quad (2)$$

$$\frac{d}{dt} \vec{\sigma}_H(t) = \frac{2v}{\hbar} \vec{\pi}_H(t) \times \vec{\sigma}_H(t) \quad (3)$$

where $\ell = \sqrt{\hbar c / |eB|}$, $(-e)B > 0$, is the magnetic length, and \vec{e}_z is the unit vector along the z -direction. The magnetic field $\vec{B} = \nabla \times \vec{A} = B\vec{e}_z$ is assumed to point along the negative z -direction, $B < 0$. The position operator $\vec{r} = (x, y)$ can be given in terms of the kinetic momentum π via the usual relations

$$x = x_0 + \frac{c}{eB} \pi_y, \quad (4)$$

$$y = y_0 - \frac{c}{eB} \pi_x, \quad (5)$$

where $\vec{r}_0 = (x_0, y_0)$ is conserved, $[\mathcal{H}, \vec{r}_0] = 0$. For cyclotron motion in a usual non-interacting two-dimensional electron gas, the vector \vec{r}_0 describes the center of the classical circular orbits. As we shall see below, this is also the case for the classical limit of cyclotron motion in graphene.

Defining the usual bosonic operators

$$a = \frac{1}{\sqrt{2}} \frac{\ell}{\hbar} (\pi_x + i\pi_y) \quad , \quad a^+ = (a)^+ \quad (6)$$

fulfilling $[a, a^+] = 1$ the Hamiltonian reads

$$\mathcal{H} = \frac{\hbar v}{\ell} \sqrt{2} (a\sigma^- + a^+\sigma^+) \quad (7)$$

where $\sigma^\pm = (\sigma^x \pm i\sigma^y)/2$. The energy scale of this Hamiltonian is given as a function of the magnetic field by

$$\frac{\hbar v}{\ell} \approx 26 \text{meV} \sqrt{\frac{B}{\text{Tesla}}}, \quad (8)$$

while its length scale is the usual magnetic length, $\ell = 257 \text{\AA} / \sqrt{B/\text{Tesla}}$. The well-known eigenstates³ of the Hamiltonian (7) are given by $|0, \uparrow\rangle$ with energy $\varepsilon_0 = 0$ and, for $n > 0$,

$$|n, \pm\rangle = \frac{1}{\sqrt{2}} (|n, \uparrow\rangle \pm |n-1, \downarrow\rangle) \quad (9)$$

with energy $\varepsilon_n^\pm = \pm(\hbar v/\ell)\sqrt{2n}$. Here n is the Landau level index, and the arrows are obvious standard notation for the sublattice spin states.

A. Numerical Approach

The operator-valued equations of motion (2), (3) do not seem to allow for a full explicit solution. However, it is straightforward though somewhat tedious to numerically evaluate the time evolution of momentum, position, and spin operators. A similar approach was performed recently in Ref.¹¹ investigating cyclotron motion in semiconductor quantum wells with spin-orbit coupling. In fact, the present case of graphene is technically clearly simpler than the previous one and was also studied very recently in Ref.¹⁰. For such numerical simulation it is convenient to work in the Landau gauge $\vec{A} = (0, Bx, 0)$ with the initial state $|\psi\rangle$ being a direct product of an orbital and a spin state,

$$|\psi\rangle = |\phi\rangle \begin{pmatrix} \kappa \\ \lambda \end{pmatrix}, \quad (10)$$

where the spinor components are related to the usual polar angles ϑ, φ of the initial pseudospin direction via $\kappa = \exp(-i\varphi/2) \cos(\vartheta/2)$, $\lambda = \exp(i\varphi/2) \sin(\vartheta/2)$. As a generic initial orbital state we consider

$$\langle \vec{r} | \phi \rangle = \frac{1}{\sqrt{\pi}d} e^{-\frac{r^2}{2d^2} + ik_0 y}, \quad (11)$$

i.e. a normalized Gaussian wave packet of spatial width d and initial momentum $\hbar k_0$ along the y -axis, i.e. the direction of translational invariance of the Hamiltonian. The initial position of the particle is at the origin, $\langle \psi | \vec{r} | \psi \rangle = 0$, and its energy is given by

$$E = \langle \psi | \mathcal{H} | \psi \rangle = \hbar v k_0 \frac{1}{\ell} (\bar{\kappa}\lambda - \kappa\bar{\lambda}) \quad (12)$$

with a quantum mechanical uncertainty of

$$\begin{aligned} (\Delta \mathcal{H})^2 &= \langle \psi | \mathcal{H}^2 | \psi \rangle - \langle \psi | \mathcal{H} | \psi \rangle^2 \\ &= \left(\frac{\hbar v}{\ell} \right)^2 \left(\frac{\ell^2}{d^2} + \frac{d^2}{2\ell^2} - (|\kappa|^2 - |\lambda|^2) \right. \\ &\quad \left. + k_0^2 \ell^2 \left(1 + (\bar{\kappa}\lambda - \kappa\bar{\lambda})^2 \right) \right) \end{aligned} \quad (13)$$

Note that the initial state (10) has in general non-vanishing overlap with single-particle eigenstates of the form (9) of both positive and negative energy. As to be discussed below, this fact leads to additional oscillations in the time evolution that can be viewed as *zitterbewegung*^{10,12,13}.

We emphasize that, by the very construction of the Hamiltonian (1), the wave number k_0 is to be interpreted relatively to the wave vector of the chosen corner of the first Brillouin zone³. The authors of Ref.¹⁰, however, consider a time evolution of an initial state of the form (10) under the simultaneous action of the Hamiltonians of both inequivalent corners of the Brillouin zone, a theoretical modeling whose physical meaning remains rather unclear. Moreover, these two Hamiltonians are assumed to differ just in a global sign, i.e. one Hamiltonian is the negative of the other, which is at odds with the microscopic tight-binding description of graphene³.

For an infinite sheet of graphene it is natural to consider initial conditions where both sublattices have the same quantum mechanical weight, $|\kappa| = |\lambda|$, i.e. the sublattice or pseudospin lies initially in its xy -plane. Fig. 1 shows several examples for numerically evaluated trajectories $\langle \vec{r}_H(t) \rangle := \langle \psi | \vec{r}_H(t) | \psi \rangle$ with this type of initial condition. For all further details of these conceptually straightforward but technically somewhat involved numerical simulations we refer to Refs.^{10,11}. In the two top panels of Fig. 1 the sublattice spin is initially collinear with the momentum. These simulations can be compared with Fig. 5 of Ref.¹⁰ where the authors consider a time evolution under a *single* Hamiltonian (not two of them) given by Eq. (1). Indeed, all results given in that figure are essentially reproduced by our own simulations underlying the present work.

The remaining panels of Fig. 1 contain simulations where the sublattice spin is in the initial state not collinear with the momentum. Note that the initial velocity $\langle \vec{v}_H \rangle = \dot{\langle \vec{r}_H \rangle}$ is determined by the initial direction of the sublattice spin via

$$\vec{v} = \frac{i}{\hbar} [\mathcal{H}, \vec{r}] = v \vec{\sigma}. \quad (14)$$

Moreover, further simulations show that there is no dynamics in the initial direction of the momentum, i.e. $\langle y_H(t) \rangle = 0$, if the sublattice spin is initially perpendicular to it, i.e. in the xz -plane. In such a case also no sublattice spin component collinear with the initial momentum develops in the time evolution, $\langle \sigma_H^y(t) \rangle = 0$. These observations were partially already made in Ref.¹⁰

and can be understood from the equations of motion (2), (3). In general, the trajectories seen in Fig. 1 are rather irregular which is a consequence of the many different excitation frequencies being present in the spectrum at low energies. In Ref.¹⁰ contributions to the time evolution involving transition frequencies between states of positive and negative energy have been regarded as an effect of *zitterbewegung*. Indeed, as to be shown below, such type of *zitterbewegung* also occurs as a correction to the classical limit.

As already mentioned in Refs.^{10,11} the numerical approach discussed above is technically limited to initial states having significant overlap with rather low Landau levels only, i.e. the method is restricted to the regime dominated by quantum effects. In the following we shall therefore explore the semiclassical limit using an analytical approach.

B. Analogy to the Jaynes-Cummings model

Further analytical progress regarding the full quantum dynamics can be made by exploiting the fact that the Hamiltonian (7) is formally equivalent to the Jaynes-Cummings model for atomic transitions in a radiation field. A similar observation has been made recently in Ref.²³ for the two-dimensional electron gas in semiconductor quantum wells with Rashba spin-orbit coupling. The Jaynes-Cummings model has been studied very intensively in theoretical quantum optics, and the time evolution of orbital and spin operators has been obtained in terms of analytical but rather implicit expressions^{26,27}. Using the method described in Refs.^{26,27} one can solve for the time-dependent position operators in the Heisenberg picture as

$$\begin{aligned} x_H(t) + iy_H(t) = & x_0 + iy_0 \\ & + \frac{ile^{-i\omega_+t}}{\omega_- - \omega_+} \left(\omega_- (\kappa_x + i\kappa_y) \ell - 2\frac{v}{\ell} \sigma^+ \right) \\ & - \frac{ile^{-i\omega_-t}}{\omega_- - \omega_+} \left(\omega_+ (\kappa_x + i\kappa_y) \ell - 2\frac{v}{\ell} \sigma^+ \right), \end{aligned} \quad (15)$$

with $\vec{\kappa} = \vec{\pi}/\hbar$, and the operator-valued frequencies ω_{\pm} are given by

$$\hbar\omega_{\pm} = -\mathcal{H} \pm \sqrt{\mathcal{H}^2 + 2 \left(\frac{\hbar v}{\ell} \right)^2}. \quad (16)$$

All operators on the r.h.s of Eq. (15) are in the Schrödinger picture, i.e. at time $t = 0$. As in the case of the two-dimensional electron gas with Rashba spin-orbit coupling investigated previously^{11,23}, the result (15) is still rather implicit and difficult to evaluate for a given initial state, mainly due to the operator character of the frequencies ω_{\pm} . However, as we shall see in next section, the above result provides a very natural access to the classical limit of the dynamics including semiclassical corrections.

III. SEMICLASSICAL LIMIT

Cyclotron motion of massful electrons is in the simplest case just described by a kinetic (effective-)mass term, and the quantum mechanical and the classical equations of motion coincide, the latter ones being the obvious and well-defined classical limit of the former. However, the classical limit of the Hamiltonian (1) describing massless fermions appears *prima vista* not as obvious. In general, the classical limit of a quantum system is approached in the limit of high energies. For our problem here this means that the energy $E = \langle \mathcal{H} \rangle$ of electron must be large compared to the characteristic energy scale $\hbar v/\ell$ of the Hamiltonian, which is equivalent to the condition $\langle \vec{\kappa} \cdot \vec{\sigma} \rangle \ell \gg 1$. In what follows we shall assume an initial state of the form (10) with momentum and sublattice spin being parallel to each other. This leads to the condition

$$k_0 \ell \gg 1. \quad (17)$$

This very natural classical limit of the graphene model in a perpendicular magnetic field corresponds to the “strong-coupling scenario” discussed in Ref.²⁵. We note that a similar limit is reached for negative energies of large modulus. Here momentum and sublattice spin are initially antiparallel.

In the limit of large energies E , the operator-valued frequencies ω_{\pm} can be replaced with classical variables,

$$\hbar\omega_{\pm} \mapsto -E \pm \sqrt{E^2 + 2 \left(\frac{\hbar v}{\ell} \right)^2}. \quad (18)$$

Then, treating also the quantities \vec{r} , \vec{r}_0 as well as $\vec{\kappa}$, $\vec{\sigma}$ as classical variables (not as operators) one derives from the full quantum result (15) in the above classical limit

$$\begin{aligned} x(t) - x_0 = & \frac{\ell}{\omega_- - \omega_+} \\ & \cdot \left[\omega_- (\kappa_x \ell \sin(\omega_+ t) - \kappa_y \ell \cos(\omega_+ t)) \right. \\ & + \frac{v}{\ell} (-\sigma^x \sin(\omega_+ t) + \sigma^y \cos(\omega_+ t)) \\ & - \omega_+ (\kappa_x \ell \sin(\omega_- t) - \kappa_y \ell \cos(\omega_- t)) \\ & \left. - \frac{v}{\ell} (-\sigma^x \sin(\omega_- t) + \sigma^y \cos(\omega_- t)) \right], \end{aligned} \quad (19)$$

$$\begin{aligned} y(t) - y_0 = & \frac{\ell}{\omega_- - \omega_+} \\ & \cdot \left[\omega_- (\kappa_x \ell \cos(\omega_+ t) + \kappa_y \ell \sin(\omega_+ t)) \right. \\ & - \frac{v}{\ell} (\sigma^x \cos(\omega_+ t) + \sigma^y \sin(\omega_+ t)) \\ & - \omega_+ (\kappa_x \ell \cos(\omega_- t) + \kappa_y \ell \sin(\omega_- t)) \\ & \left. + \frac{v}{\ell} (\sigma^x \cos(\omega_- t) + \sigma^y \sin(\omega_- t)) \right]. \end{aligned} \quad (20)$$

Again the quantities $\vec{\kappa}$, $\vec{\sigma}$ in the rectangular brackets on the r.h.s. are at time $t = 0$. Moreover, in the classical limit $E \gg \hbar v/\ell$ we have $\hbar\omega_- \approx -2E$ and $\hbar\omega_+ \approx (\hbar v/\ell)^2/E$. It is instructive to rewrite the latter expression in the usual form of a cyclotron frequency $\hbar\omega_+ =: \omega_c = |eB|/m_c$. Here the cyclotron mass is given by the well-known semiclassical expression^{4,28} $m_c = (\hbar^2/2\pi)\partial S/\partial E = E/v^2$ where $S = \pi k_0^2$ is the area enclosed by a cyclotron orbit, and $E = \hbar v k_0$. Now, expanding the above expressions in first order in $(\hbar v/\ell)/E$ one finds

$$\begin{aligned} x(t) - x_0 &= \kappa_x \ell^2 \sin(\omega_c t) - \kappa_y \ell^2 \cos(\omega_c t) \\ &+ \frac{\hbar v}{E} \left(-\sigma^x \sin(\omega_c t) + \sigma^y \cos(\omega_c t) \right. \\ &\quad \left. - \sigma^x \sin(2Et/\hbar) - \sigma^y \cos(2Et/\hbar) \right), \end{aligned} \quad (21)$$

$$\begin{aligned} y(t) - y_0 &= \kappa_x \ell^2 \cos(\omega_c t) + \kappa_y \ell^2 \sin(\omega_c t) \\ &- \frac{\hbar v}{E} \left(\sigma^x \cos(\omega_c t) + \sigma^y \sin(\omega_c t) \right. \\ &\quad \left. - \sigma^x \cos(2Et/\hbar) + \sigma^y \sin(2Et/\hbar) \right). \end{aligned} \quad (22)$$

The first lines of the above r.h.s. describe the classical cyclotron motion^{11,28} with an energy-dependent cyclotron mass⁴. The other contribution are lowest-order semiclassical corrections to this classical limit. In particular, the terms in the last lines oscillate with the large frequency $2E/\hbar \gg \omega_c$ which equals the energy separation $2E = 2\hbar v k_0$ between states of positive and negative energy at given wave vector in the absence of a magnetic field³. Therefore, these semiclassical correction can be viewed as an effect of *zitterbewegung*^{10,12,13}. We note that in connection with graphene the term “*zitterbewegung*” was also used recently to express the fact that the velocity operator (14) fails to commute with the Hamiltonian (1)²⁹.

So far we have concentrated on semiclassical dynamics at large positive energies $E \gg \hbar v/\ell$. In the analogous case of negative energies of large modulus one obtains a similar result with the frequencies ω_{\pm} being interchanged, $\omega_+ \approx 2|E|$, $\omega_- \approx -\omega_c$.

Finally we note the equivalence of the following three conditions:

$$E \gg \hbar\omega_c = \frac{(\hbar v)^2}{E} \quad (23)$$

$$\Leftrightarrow E^2 = (\hbar v k_0)^2 \gg \left(\frac{\hbar v}{\ell}\right)^2 \quad (24)$$

$$\Leftrightarrow (k_0 \ell)^2 \gg 1 \quad (25)$$

Thus, the condition (23) is fulfilled whenever (17) is valid.

On the other hand, the condition (17) can be rewritten as $r_c \gg \ell$ with $r_c = k_0 \ell^2$ being the classical cyclotron radius. This is indeed the usual textbook criterion for the validity of semiclassical approximations to cyclotron dynamics in solids²⁸ and confirms again our above strategy of obtaining the semiclassical limit.

Let us now compare our results with the Shubnikov-de Haas measurements by Novoselov *et al.*⁴. The data presented in Fig. 2a of Ref.⁴ was obtained at an electron density of $n \approx 4.3 \cdot 10^{12} \text{cm}^{-2}$ and magnetic fields of up to about $B = 10 \text{T}$, corresponding to a Fermi wave vector of $k_f = \sqrt{\pi n} \approx 3.7 \cdot 10^6 \text{cm}^{-1}$ and a magnetic length of $\ell \gtrsim 81 \text{\AA}$. Thus, $k_f \ell \gtrsim 3$, and the criterion (17) is still reasonably fulfilled even for the highest fields used in those measurements. Correspondingly, we have $(\hbar v/\ell)/E \lesssim 0.33$ with $E = \hbar v k_f$, showing that the semiclassical correction obtained in Eqs. (21),(22) are sufficiently suppressed which allows for an interpretation of the experimental data in purely classical terms. At higher magnetic fields, quantum effects dominate, and quantized Hall transport is observed^{4,5,6}.

IV. CONCLUSIONS

We have investigated cyclotron motion in graphene monolayers considering both the full quantum dynamics and its semiclassical limit obtained for high carrier energies. At low energies, the quantum dynamics leads to rather irregular particle trajectories dominated by effects of *zitterbewegung* due to the two dispersion branches of the spectrum. The semiclassical limit of the system is obtained using the analogy of the Hamiltonian with the Jaynes-Cummings model^{11,23}. A similar analysis of the classical limit can be done for cyclotron motion in semiconductor quantum wells with spin-orbit interaction^{11,23}. The semiclassical limit of cyclotron dynamics in graphene is described by the usual cyclotron frequency and the characteristic frequency of *zitterbewegung* which occurs as a semiclassical correction. Recent experiments are shown to operate in the semiclassical regime.

Acknowledgments

I thank M. I. Katsnelson, M. Trushin, and U. Zülicke for useful discussions. This work was supported by DFG via SFB 689 “Spin Phenomena in reduced Dimensions”.

¹ K. S. Novoselov, A. K. Geim, S. V. Morozov, D. Jiang, Y. Zhang, S. V. Dubonos, I. V. Grigorieva, and A. A. Firsov, *Science* **306**, 666 (2004).

² A. K. Geim and K. S. Novoselov, *Nature Mat.* **6**, 183

(2007).

³ A. H. Castro Neto, F. Guinea, N. M. R. Peres, K. S. Novoselov, and A. K. Geim, arXiv:0709.1163.

⁴ K. S. Novoselov, A. K. Geim, S. V. Morozov, D. Jiang,

- M. I. Katsnelson, I. V. Grigorieva, S. V. Dubonos, and A. A. Firsov, *Nature* **438**, 197 (2005).
- ⁵ Y. Zhang, Y.-W. Tan, H. L. Stormer, and P. Kim, *Nature* **438**, 201 (2005).
- ⁶ K. S. Novoselov, Z. Jiang, Y. Zhang, S. V. Morozov, H. L. Stormer, U. Zeitler, J. C. Maan, G. S. Boebinger, P. Kim, and A. K. Geim, *Science* **315**, 1379 (2007).
- ⁷ R. S. Deacon, K.-C. Chuang, R. J. Nicholas, K. S. Novoselov, and A. K. Geim, *Phys. Rev. B* **76**, 081406 (2007).
- ⁸ Z. Jiang, E. A. Henriksen, L. C. Tung, Y.-J. Wang, M. E. Schwartz, M. Y. Han, P. Kim, and H. L. Stormer, *Phys. Rev. Lett.* **98**, 197403 (2007).
- ⁹ Z. Jiang, Y. Zhang, H. L. Stormer, and P. Kim, *Phys. Rev. Lett.* **99**, 106802 (2007).
- ¹⁰ T. M. Rusin and W. Zawadzki, arXiv:0712.3590v1.
- ¹¹ J. Schliemann, arXiv:0710.5395v2.
- ¹² J. Schliemann, D. Loss, and R. M. Westervelt, *Phys. Rev. Lett.* **94**, 206801 (2005).
- ¹³ J. Schliemann, D. Loss, and R. M. Westervelt, *Phys. Rev. B* **73**, 085323 (2006).
- ¹⁴ W. Zawadzki, *Phys. Rev. B* **72**, 085217 (2005); *Phys. Rev. B* **74**, 205439 (2006).
- ¹⁵ B. K. Nikolic, L. P. Zarbo, and S. Welack, *Phys. Rev. B* **72**, 075335 (2005).
- ¹⁶ S.-Q. Shen, *Phys. Rev. Lett.* **95**, 187203 (2005).
- ¹⁷ J. Cserti and G. David, *Phys. Rev. B* **74**, 172305 (2006).
- ¹⁸ P. Brushein and H. Q. Xu, *Phys. Rev. B* **74**, 205307 (2006).
- ¹⁹ T. M. Rusin and W. Zawadzki, *J. Phys.: Condens. Mat.* **19**, 136219 (2007).
- ²⁰ B. Trauzettel, Y. M. Blanter, and A. F. Mopurgo, *Phys. Rev. B* **75**, 035305 (2007).
- ²¹ T. M. Rusin and W. Zawadzki, *Phys. Rev. B* **76**, 195439 (2007).
- ²² J. Schliemann, *Phys. Rev. B* **75**, 045304 (2007).
- ²³ R. Winkler, U. Zülicke, and J. Bolte, *Phys. Rev. B* **75**, 205314 (2007).
- ²⁴ E. Bernardes, J. Schliemann, M. Lee, J. C. Egues, and D. Loss, *Phys. Rev. Lett.* **99**, 076603 (2007).
- ²⁵ U. Zülicke, J. Bolte, and R. Winkler, *New J. Phys.* **9**, 355 (2007).
- ²⁶ J. R. Ackerhalt and K. Rzazewski, *Phys. Rev. A* **12**, 2549 (1975).
- ²⁷ S. M. Barnett and P. M. Radmore, *Methods in Theoretical Quantum Optics*, Clarendon Press, Oxford 1997.
- ²⁸ N. W. Ashcroft and N. D. Mermin, *Solid State Physics*, Thomson 1976.
- ²⁹ M. I. Katsnelson, *Eur. Phys. J.* **51**, 157 (2006).

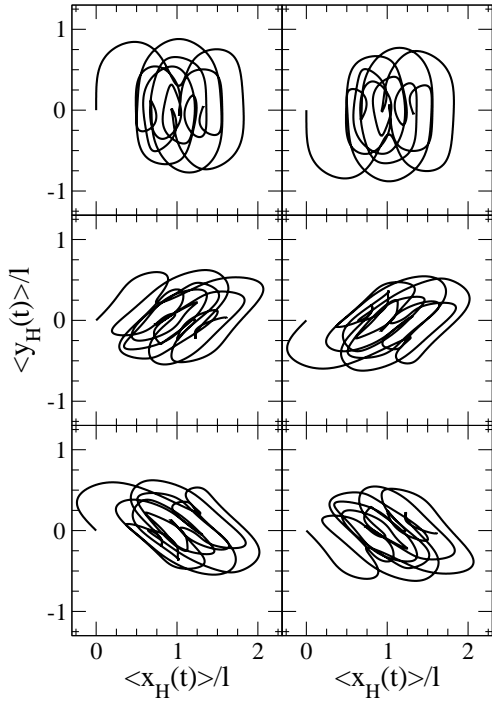


FIG. 1: Orbital dynamics of a wave packet of initial width $d = 1.0\ell$ and group wave number $k_0 = 1.0/\ell$. In all cases the sublattice spin lies initially in the xy -plane, i.e. $\vartheta = \pi/2$ leading to $|\kappa| = |\lambda|$, and the total simulation time is always $50\ell/v$. In the left and right top panel, the sublattice spin is initially collinear with the momentum with $\varphi = \pi/2$ and $\varphi = 3\pi/2$, respectively. In the middle panels we have $\varphi = \pi/4$ (left) and $\varphi = 5\pi/4$ (right) as initial conditions, while in the bottom panels $\varphi = 3\pi/4$ and $\varphi = 7\pi/4$ were used